Probiotics and Antimicrobial Proteins
https://doi.org/10.1007/s12602-025-10866-y

RESEARCH

Therapeutic Potential of Antimicrobial Peptide Scymicrosin$_{7\text{-}26}$ against the Emerging Pathogen *Acinetobacter ursingii* Isolated from *Litopenaeus vannamei*

Ying Wang[1,2] · Hanxiao Li[1,2] · Hua Hao[1,2,3] · Ying Zhou[1,2] · Fangyi Chen[1,2,3] · Ke-Jian Wang[1,2,3]

Received: 9 September 2025 / Accepted: 20 November 2025

Abstract

The Pacific white shrimp (*Litopenaeus vannamei*) aquaculture faces emerging threats from novel pathogens and escalating antibiotic resistance. This study successfully isolated and identified the pathogenic bacterium *Acinetobacter ursingii* strain 31C2 from diseased *L. vannamei* using an integrated approach combining microbiological, biochemical, and molecular techniques. The pathogenicity of this strain was confirmed in *L. vannamei* and marine medaka (*Oryzias melastigma*) infection models, exhibiting a strong dose-dependent mortality, with median lethal doses (LD_{50}) of 2.83×10^4 CFU/g shrimp and 2.58×10^6 CFU/fish, respectively. Infection caused severe hepatopancreatic necrosis (tubular deformation and epithelial vacuolation) and intestinal villi destruction. Antimicrobial susceptibility testing revealed that the 31C2 strain was resistant to tetracycline and azithromycin. To identify effective agents targeting this strain, the antimicrobial peptide Scymicrosin$_{7\text{-}26}$ (derived from *Scylla paramamosain*) was evaluated. The peptide had potent antibacterial activity against *A. ursingii* 31C2 in vitro (MIC: 3–6 μM). In vivo application significantly enhanced survival of *L. vannamei* and *O. melastigma* infected with 31C2 by 30% and 20%, respectively. Treatment drastically reduced bacterial loads in the hepatopancreas and intestine, restored tissue integrity, and modulated the immune response by suppressing the hyperactivation of the Toll and IMD pathways and their downstream transcription factors, *dorsal* and *relish*, while upregulating *penaeidin3* and *propo* expression. This study identified *A. ursingii* as an emerging shrimp pathogen and validated Scymicrosin$_{7\text{-}26}$ as a promising antibiotic-free therapeutic for disease control in aquaculture.

Keywords *Acinetobacter Ursingii* 31C2 · Pathogenicity · Litopenaeus vannamei · Antimicrobial peptide · Scymicrosin$_{7\text{-}26}$ · Therapeutic strategy

Introduction

The Pacific white shrimp, also known as *Penaeus vannamei* or *Litopenaeus vannamei*, is indigenous to the coastal waters of the Pacific Ocean in the Americas [1]. Owing to its rapid growth rate, high nutritional value, and strong environmental adaptability, *L. vannamei* has become the dominant cultured crustacean species worldwide, contributing approximately 53.3% (6.8 million tons) of global farmed crustacean production in 2022, highlighting its crucial role in global aquaculture [2]. China holds the distinction of being the leading nation in the culturing and production of *L. vannamei*. As reported by the Ministry of Agriculture and Rural Affairs of the People's Republic of China (MARA), *L. vannamei* represented approximately 80.9% of the overall shrimp culture output in China for the year 2023,

Ying Wang and Hanxiao Li contributed equally to this work.

✉ Fangyi Chen
chenfangyi@xmu.edu.cn

✉ Ke-Jian Wang
wkjian@xmu.edu.cn

1 State Key Laboratory of Marine Environmental Science, College of Ocean & Earth Sciences, Xiamen University, Xiamen 361102, China

2 State-Province Joint Engineering Laboratory of Marine Bioproducts and Technology, College of Ocean & Earth Sciences, Xiamen University, Xiamen 361102, China

3 Marine Biological Antimicrobial Peptide Industry Research Institute, Fujian Ocean Innovation Center, Xiamen 361102, China

Published online: 05 December 2025

establishing it as the predominant shrimp species cultivated in the country [3]. With the increasing demand for shrimp and the development of shrimp farming industry, the level of intensive culture of *L. vannamei* is steadily rising. However, in the process of intensive aquaculture, challenges such as high stocking densities, deteriorating water quality, and severe diseases have emerged, greatly constraining shrimp aquaculture development [4–6]. Bacterial disease problems are often a significant contributor to economic losses among the various influencing factors. For example, infections caused by *Vibrio* and *Aeromonas* spp. can lead to massive mortality of shrimp [7–13]. Meanwhile, a growing number of new pathogenic microorganisms have been identified in marine animal diseases, including *Kocuria* spp., *Nocardia* spp., *Francisella* spp., and *Mycobacterium* spp [14].

Acinetobacter spp. is a class of non-fermentative, oxidase-negative, catalase-positive and non-motile Gram-negative coccobacilli, widely distributed in soil, ponds, skin, airway, gastrointestinal tract and other environments of animals, including humans [15–18]. The short rod-shaped (coccobacillary) morphology is a defining phenotypic feature of the genus *Acinetobacter*, distinguishing it from other Gram-negative bacteria such as *Pseudomonas* or *Aeromonas*. *Acinetobacter* is a common pathogenic bacterium in medical clinics, which can cause diseases such as pneumonia, meningitis and cholangitis in humans [19, 20]. *Acinetobacter ursingii* belongs to the genus *Acinetobacter* and was described as a new species in 2001 [21, 22]. It is generally considered an opportunistic pathogen capable of causing serious infections including bloodstream infections (bacteremia) [23]. *A. ursingii* can cause urinary tract infections in canines [24]. Its infection leads to clinical signs such as discoloration of the body surface, fin ray erosion, spleen enlargement and intestinal inflammation in *Oncorhynchus mykiss* [25]. To date, only one case of *A. ursingii* infection has been reported in *O. mykiss*, and there have been no reports in shrimp. Based on the currently available information, reports of *A. ursingii* infections in aquatic animals are very limited. However, this does not mean that *A. ursingii* is not present or non-pathogenic in shrimp; it may simply be that insufficient attention has been paid or there is a lack of corresponding research to date. Advances in the pathogenesis of *A. ursingii*, host immune response, prevention and treatment strategies are crucial for the development of effective disease management measures. Meanwhile, the increasing number of bacterial infections poses a major threat to the development of the aquaculture industry and human health. Antibiotic resistance caused by the misuse of antibiotics is widespread in animals and the environment, and the risk of spreading antibiotic resistance to humans is increasing [26, 27]. It is crucial to seek out possible alternatives to antibiotics for treating microbial infections in order to reduce the rise and dissemination of antibiotic-resistant bacteria.

Antimicrobial peptides (AMPs) are small, positively charged, amphipathic molecules that demonstrate extensive antimicrobial effectiveness against various pathogens, encompassing bacteria, fungi, viruses, and parasites [28]. They are part of the innate immune system and are found in various organisms, such as mammals, insects, plants, and bacteria [29]. AMPs are characterized by their diverse structures, which can be classified into several categories, including α-helical, β-sheet, and looped peptides, some of which lack a defined secondary structure [30]. AMPs have cationic and hydrophobic properties, and are capable of interacting with microbial cell membranes, causing membrane disruption or dysfunction, thereby inhibiting or killing pathogens [31, 32]. Currently, more and more pathogens are becoming resistant to traditional antibiotics, and the development of AMPs as new anti-infective agents has attracted much attention. AMPs not only possess a broad-spectrum antimicrobial activity, but also have a lower capacity to induce drug resistance than antibiotics, thus offering potential advantages in the treatment of difficult to control infections [31, 32]. In addition, AMPs can modulate the host's immune response, acting as signaling molecules to activate or enhance the host's innate and adaptive immune responses [29, 31, 33]. Therefore, AMPs are very promising alternatives to antibiotics. To address the escalating drug resistance crisis, discovering novel AMPs from natural sources represents a key approach. Among these natural sources, marine organisms serve as a vital reservoir for screening new AMPs. A series of novel AMPs have previously been identified from various marine species by the research group. For instance, Scygonadin, an anionic antimicrobial peptide first isolated and purified from the gonads of *Scylla paramamosain*, can be efficiently expressed in the *Pichia pastoris* system [34]. The recombinantly produced Scygonadin exhibits significant antibacterial activity against Gram-positive bacteria (such as *Micrococcus lysodeikticus* and *Staphylococcus aureus*) and Gram-negative bacteria (such as *Aeromonas hydrophila*). Similarly, Spgillcin$_{177-189}$, another peptide derived from *S. paramamosain*, demonstrates broad-spectrum bactericidal activity and shows a lower tendency to induce bacterial resistance [35]. Furthermore, Scymicrosin$_{7-26}$ from *S. paramamosain* and Bolespleenin$_{334-347}$ from *Boleophthalmus pectinirostris* both possess broad-spectrum bactericidal capabilities and exhibit significant therapeutic efficacy against local skin infections caused by methicillin-resistant *Staphylococcus aureus* (MRSA) [29, 36].

In this study, *A. ursingii* was isolated from diseased *L. vannamei* for the first time using conventional microbial culture techniques as the primary approach. Through systematic isolation, identification and pathogenicity assessment, the study aimed to clarify the pathogenic mechanism of this emerging pathogen *A. ursingii* on *L. vannamei*.

Furthermore, using a laboratory-established AMP database, four candidate peptides (Scygonadin, Bolespleenin$_{334–347}$, Spgillcin$_{177–189}$ and Scymicrosin$_{7–26}$) were screened for in vitro antibacterial activity. Scymicrosin$_{7–26}$ demonstrated potent inhibition against *A. ursingii*, prompting further investigation into its therapeutic potential using in vivo infection models. These findings establish a foundational framework for developing novel AMP-based therapeutics against emerging pathogens in shrimp aquaculture.

Materials and Methods

Experimental Animals

Diseased *L. vannamei*: In November 2021, several instances of mortality were observed in *L. vannamei* at a shrimp farm in Zhangpu County, Fujian Province, China. Prior to death, the diseased shrimp displayed clinical signs including sluggish movement and decreased appetite. Six moribund *L. vannamei* (12.18 ± 3.74 g) were sampled for examination of external lesions, ectoparasite detection, and bacterial isolation.

L. vannamei for experiment: Healthy *L. vannamei* (19.47 ± 1.55 g) were obtained from a shrimp farm in Xiamen, Fujian Province, China, and placed in a 300 L culture tank sterilized and filled with artificial seawater beforehand. The salinity of the artificial seawater was 30‰, and the culturing temperature was 28 ± 1 °C. The water quality was maintained in good condition, with half of the seawater replaced every day, dissolved oxygen ≥ 6.0 mg/L, and the dead or slow-moving shrimp were promptly removed. During the acclimation, all shrimp were fed a commercial formulated diet (Guangdong Yuehai Feed Group Co., Ltd., China) twice daily at 08:00 and 18:00. The feeding rate was adjusted to approximately 3–5% of the total body weight per day according to their feeding activity, uneaten feed and feces were removed after each feeding to ensure high water quality standards.

Marine medaka for experiment: The marine medaka (*O. melastigma*) have been stably bred for more than 10 generations at the Marine Medaka Breeding Center, College of Ocean and Earth Sciences, Xiamen University. Healthy 3-month-old individuals with an average body weight of 0.33 ± 0.02 g were selected for the experiments. Culture conditions: artificial seawater salinity of 30‰, culturing temperature of 28 ± 1 °C, light control starting at 08:00 and ending at 22:00 every day to simulate the photoperiod (day-night ratio of 14:10), and the medaka were fed twice a day with brine shrimp at 09:00 and 17:00. Before the experiment, they were acclimated for more than 48 h without feeding.

Bacterial Isolation and Identification

The surfaces of the diseased *L. vannamei* underwent a disinfection process using cotton balls soaked in 75% alcohol. Sterile scissors and forceps were used to dissect the shrimp, and tissues including the hepatopancreas, intestine, stomach, gills, eyes, muscle, and heart were collected and ground in sterile physiological saline. The ground tissues were then diluted into 10^{-1}, 10^{-2}, 10^{-3}, and 10^{-4} dilutions with a gradient of 1:9 in physiological saline, and each dilution was inoculated onto sterile brain heart infusion (BHI) medium (Difco Becton Dickinson) agar plates in triplicate. After incubation at 37 °C for 24 h, single colonies with different morphologies and sizes were selected for picking and purification on BHI agar plates, followed by cultivation in liquid BHI medium at 37 °C for 24 h (180 rpm). The bacterial suspension was mixed with a sterile 50% (v/v) glycerol solution at a ratio of 6:4 and stored at −80 °C for long-term preservation. The isolated bacterial strains were inoculated onto 10% defibrinated sheep blood agar plates (Huankai, Guangzhou, China) and were incubated at 37 °C for 24 h to assess hemolytic activity.

Bacteria with hemolytic activity were classified after Gram staining. Genomic DNA was extracted using the bacterial genomic DNA extraction kit (Qiagen), and PCR amplification was performed using 16 S rRNA primers (27 F and 1942R) and specific primers for the bacterial *rpob* gene [37]. The primer sequences are listed in Table S1. The 30 μL reaction system consisted of 12 μL of ddH_2O, 15 μL of primer mix, 1 μL of template and 1 μL each of forward and reverse primers. Sequencing of the PCR products was performed by Sangon Biotech (Shanghai) Co., Ltd. The obtained 16 S rRNA gene sequences were analyzed using BLASTn against the NCBI GenBank nucleotide database to identify the closest phylogenetic relatives. A multiple sequence alignment was conducted using ClustalW, and a phylogenetic tree was constructed in MEGA 6.0 using the neighbor-joining method with 1,000 bootstrap replications. Additionally, biochemical identification of the single bacterial strains was performed using biochemical identification tubes (Huankai, Guangzhou, China), referring to the "Bergey's Manual of Determinative Bacteriology" [38].

Experimental Infection and Determination of the Median Lethal Dose (LD50)

Healthy shrimp used for infection experiments were sourced from the same batch described in Section Experimental animal. Prior to infection, all shrimp were acclimated for seven days under the same conditions (28 ± 1 °C, salinity 30 ± 1‰, dissolved oxygen >6 mg/L, pH 7.8 ± 0.2), as detailed in Section Experimental animal. Each

group consisted of three replicate tanks (60 L each), with 20 shrimp per replicate. After acclimation, the bacterial suspension was prepared from *A. ursingii* strain 31C2 cultured in brain heart infusion (BHI) broth at 37 °C for 18–24 h until reaching the logarithmic growth phase. The bacterial cells were harvested by centrifugation at 5000 × g for 10 min, washed twice with sterile normal saline, and resuspended in sterile normal saline to the desired concentration. The concentration of the bacterial suspension was then determined using the plate counting method [39, 40]. Briefly, serial 10-fold dilutions were prepared with sterile normal saline, and 100 µL aliquots of each dilution were spread onto BHI agar plates. After incubation at 37 °C for 24 h, visible colonies were counted, and the viable bacterial concentration (CFU/mL) was calculated as the mean of triplicate plates. The bacterial suspension was subsequently adjusted to concentrations ranging from 10^4 to 10^8 CFU/mL for preliminary infection trials, and based on the resulting mortality data, the optimal bacterial dose was selected for subsequent infection experiments to ensure reproducibility and a moderate infection intensity. Healthy shrimp with uniform size (16.18 ± 2.3 g) were selected for the experiment, which included a negative control group (NC), and three experimental groups (A, B, and D), with three replicates of 20 shrimp each. Groups A, B, and D were intramuscularly injected into the fifth abdominal segment with 4.16×10^4, 4.16×10^5, and 4.16×10^6 CFU/g body weight, respectively. The NC group received an equal volume of sterile physiological saline injection. The vitality, clinical signs, and mortality of the shrimp in the experimental and NC groups were continuously observed, and the dead individuals were promptly removed. Survival rates were recorded, and moribund shrimp were dissected to examine internal lesions. Bacteria were re-isolated from infected tissues to confirm pathogen identity. The LD_{50} of the bacterial strain was calculated using the modified Karber method [41].

After a 48-h acclimation period for the medaka, healthy fish with uniform size were selected for the experiment, which included a NC and five experimental groups (OM-A, OM-B, OM-C, OM-D, and OM-E), with three replicates of 30 fish each. The concentration of the bacterial suspension was calculated using the plate counting method. Groups OM-A, OM-B, OM-C, OM-D, and OM-E were intraperitoneally injected with 1×10^6, 10^7, 10^8, 10^9, and 10^{10} CFU/mL of the bacterial strain, respectively, at a rate of 8.8 µL per fish. The NC groups received an equal volume of sterile physiological saline injection (OM-NC). The vitality, disease, and mortality of the medaka in the experimental and NC groups were continuously observed, and dead fish were promptly removed. The survival rate was recorded, and the LD_{50} was calculated.

Pathogen Susceptibility Testing and *in vitro* Antimicrobial Peptide Inhibition Assay

First, isolated bacterial strains were streaked onto MH agar plates and incubated at 37 °C for a duration of 16 to 24 h to acquire monoclonal colonies. Following this, these monoclonal colonies were transferred into 1 mL of MH liquid medium and cultivated at 37 °C for 4 h under agitation at 180 rpm for future experiments. The turbidity of the resulting bacterial suspension was then modified to achieve a McFarland standard of 0.5 to 0.6 using a McFarland turbidity standard tube. Subsequently, the bacterial suspension was spread evenly on MH solid agar plates under sterile conditions, and the plates were left at room temperature for 2–3 min. Test strips for antimicrobial susceptibility (OXOID, England) were subsequently placed on the plates and incubated at a temperature of 37 °C for 24 h. Upon completion of the incubation period, the diameters of the inhibition zones were assessed with a caliper. The interpretation of antimicrobial susceptibility results was carried out in accordance with the Clinical and Laboratory Standards Institute (CLSI) guidelines [42].

Several newly identified AMPs, including Scygonadin1, $Spgillcin_{177–189}$, $Bolespleenin_{334–347}$, and $Scymicrosin_{7–26}$, which had been previously characterized in earlier studies, were chemically synthesized. The in vitro antibacterial assay was conducted against the isolated *A. ursingii* using the broth microdilution method with slight modifications [26]. Initially, the monoclonal bacterial strain was inoculated into the BHI liquid medium and cultured to logarithmic phase. It was then diluted to 10^6 CFU/mL, followed by low-speed centrifugation. The pellet was resuspended in BHI liquid medium. Concurrently, the synthetic peptides were diluted with sterile water to concentrations of 48, 24, 12, 6, 3, 1.5, 0.75, and 0.375 µM and stored at 4 °C for later use. An NC group (50 µL of the antimicrobial peptide to be tested + 50 µL of sterile water), a positive control group (50 µL of sterile water + 50 µL of bacterial suspension), and experimental groups with different concentrations (50 µL of the antimicrobial peptide to be tested + 50 µL of bacterial suspension) were prepared. The mixtures were thoroughly mixed and incubated in a culture chamber for 24 h to observe the minimum inhibitory concentration (MIC). The mixtures from transparent wells were spread onto BHI agar plates and incubated at 37 °C for 24 h. The presence or absence of bacterial growth was then recorded to determine the minimum bactericidal concentration (MBC). Each group had three replicates, and the independent experiment was repeated twice.

Scanning Electron Microscopy (SEM) Observation

SEM sample processing followed established protocols with modifications [36]. First, bacterial strains were activated, enriched and cultivated to logarithmic growth phase. After centrifugation, the supernatant was discarded, and the bacterial pellet was resuspended in MH medium, adjusted an absorbance at the optical density (OD) 600 nm to 0.2. Then, 500 µL of the bacterial suspension was mixed with an equal volume of 6 µM Scymicrosin$_{7-26}$ solution to reach a final concentration of 3 µM. The exposure time of 30 min was determined through preliminary optimization experiments, which showed that this duration was sufficient to induce visible surface disruption of *A. ursingii* cells under SEM, while longer exposures caused excessive cellular collapse and obscured morphological details. They were then co-incubated at 37 °C for 30 min, centrifuged to remove the supernatant, washed once with PBS, and fixed overnight at 4 °C with 2.5% glutaraldehyde. After washing three times with PBS, the bacterial pellet was resuspended in 10 µL of PBS, dropped onto pre-cut glass slides, and allowed to adhere for 30 min. Excess liquid was absorbed with filter paper, and the samples were subjected to a gradient dehydration process with ethanol at concentrations of 30%, 50%, 70%, 80%, 95%, and 100% for 5 min, 5 min, 10 min, 10 min, 15 min, and 15 min respectively. After a second treatment with 100% ethanol for 15 min, the samples were subjected to critical point drying. After gold sputtering, the samples were observed and photographed using a scanning electron microscopy (FEI Quanta 650 FEG, United States).

The Anti-infective Effect of Scymicrosin$_{7-26}$ on *L. vannamei* and *O. melastigma* Infected with *A. ursingii* 31C2

After a 7-day preliminary culture, healthy shrimp with robust physique and uniform size (19.47 ± 1.55 g) were selected for the experiment. The challenge experiment was designed in different groups, including NC group (PV+PBS+PBS), an infection group (PV+A.U+PBS), and AMP treatment group (PV+A.U+Scymicrosin$_{7-26}$), with three replicates of 20 shrimp each. The infection group and AMP treatment group were injected intramuscularly with LD_{50} of *A. ursingii* at 25 µL per shrimp in the fifth abdominal segment of the *L. vannamei*. The AMP treatment group was injected with the same dose of 1.5 mg/mL of Scymicrosin$_{7-26}$ 1 h after infection. The NC and infection groups were injected with the same volume of sterile PBS. No food was fed during the challenge period and normal aeration was provided. The vitality, disease, and death of the *L. vannamei* in the experimental and NC groups were continuously observed, and dead shrimp were promptly removed.

Adopting the challenge methodology established for *L. vannamei*, healthy three-month-old *O. melastigma* exhibiting robust physique and uniform size were selected after a 48-h preliminary culture. The trial was designed with an NC group (OM+PBS+PBS), an infection group (OM+A.U+PBS), and the AMP treatment group (OM+A.U+Scymicrosin$_{7-26}$), with three replicates of 20 fish each. The infection group and AMP treatment group were injected intraperitoneally with the LD_{50} dose of *A. ursingii* at 8.8 µL per fish.

Bacterial Load

After injection of *A. ursingii* 31C2, liver and intestinal samples were collected from each group of shrimp and *O. melastigma* at various time points (3, 6, 9, 12, 24, and 48 h). The tissues were homogenized, followed by gradient dilution and then spread on BHI agar plates. The bacterial load per gram of tissue was assessed using the plate counting method.

Histopathological Observation

After infection with *A. ursingii* 31C2 at different time points (3, 6, 9, 12, 24, and 48 h), liver, gut, and other samples of each group of shrimp and *O. melastigma* were fixed in 4% paraformaldehyde. The solution was changed every 24 h. The samples underwent dehydration, clarification, wax embedding, sectioning, mounting, deparaffinization, staining, ethanol gradient dehydration, and sealing to complete the preparation of hematoxylin and eosin (H&E) stained Sects [36, 43]. Electron microscopy (Mingmei Optoelectronics Technology Co., Ltd., Guangzhou, China) was used for section observation.

Expression of Immune-Related Genes

The hepatopancreas and intestinal tissues of *L. vannamei* and *O. melastigma* were placed into 2 mL grinding tubes preloaded with 1 mL of RNase-free TRIzol reagent and homogenized thoroughly using a low-temperature tissue grinder. The homogenates were left at room temperature for 5–10 min, and total RNA was then extracted from the tissues using the TRIzol method [44]. The quality of the total RNA was detected by 1.2% (w/v) agarose gel electrophoresis, and the concentration and purity were measured using the Nanodrop 2000 ultra-micro-UV-Vi's spectrophotometer (Thermo Fisher Scientific Inc., United States). The genomic DNA was removed using Promega DNase, and the extracted total RNA was reverse transcribed using the PrimerScript™ RT-PCR kit (Perfect Real Time) to obtain cDNA, which was stored at −20 °C for later use. The sequences of the relevant

primers can be found in Table S2. Changes in the expression of immune-related genes in Scymicrosin$_{7-26}$-treated shrimp challenged with *A. ursingii* 31C2 were analyzed by quantitative real-time PCR (qRT-PCR). The target genes evaluated included components of the immune signaling pathways (such as *toll*, *imd*, *relish*, and *dorsal*), the enzyme involved in the melanization cascade (prophenoloxidase, *propo*), and antimicrobial effector molecules (including Anti-lipopolysaccharide factor, *alf*; *crustin*; and *penaeidin3*). Internal reference genes utilized were *β-actin* and elongation factor 1-alpha (*ef-1α*). Expression profiles were determined using the $2^{-\Delta\Delta Ct}$ method [45]. A total of six independent biological replicates were conducted for all experiments.

Statistical Analysis

Statistical analyses were performed using GraphPad Prism 9.0 (GraphPad Software, Inc., USA) and SPSS 22.0 (IBM Corp., USA). Prior to analysis, data were tested for normality using the Shapiro–Wilk test and for homogeneity of variances using Levene's test. Differences among groups were analyzed by one-way analysis of variance (ANOVA) followed by Tukey's multiple range test for post hoc comparisons. All results are presented as mean ± standard deviation (SD), and statistical significance was accepted at $p < 0.05$. Different letters or asterisks in the figures indicate significant differences among treatments.

Results

Clinical Signs of Diseased *L. vannamei*

The diseased shrimp exhibited reduced vitality, sluggish movement, broken antennae and appendages, and reddish tail fans and pleopods, with the presence of black spots on the body surface. Upon dissection, the hepatopancreas showed localized degeneration and discoloration, while the intestines appeared reddened, thinned, and fragile. No parasites were observed on the body surface or within the body cavity (Fig. S1).

Isolation and Identification of Candidate Pathogens from Diseased *L. vannamei*

From various tissues of six diseased shrimp, a total of 119 pure bacterial cultures were isolated and purified. They were spotted on blood agar plates and incubated at 37 °C for 24 h. Among them, 23 strains exhibited β-hemolytic activity. Through 16 S rRNA sequencing, six types of hemolytic bacteria were identified at the genus level (Fig. 1A), including 11 strains of *Aeromonas*, one strain of *Exiguobacterium*, 5 strains of *Stenotrophomonas*, 3 strains of *Bacillus*, 2 strains of *Acinetobacter*, and one strain of *Pseudomonas*. Most of these hemolytic bacteria are potentially pathogenic. Upon further identification, the study found a strain of *Acinetobacter*, named 31C2, which has never been reported in shrimp. This bacterium showed Gram-negative characteristics after Gram staining (Fig. 1B). Biochemical identification results (Table 1) indicated that the strain was positive for catalase and Simmons' citrate, negative for oxidase, unable to utilize glucose, lactose, maltose, sucrose, mannose, sorbitol, and arabinose, unable to hydrolyze esculin, negative for nitrate reduction, and unable to spread in semi-solid agar. This isolate possesses the basic characteristics of the *Acinetobacter* genus, being a non-fermentative, non-motile, oxidase-negative, catalase-positive, and Simmons' citrate-positive Gram-negative bacterium. The 16 S rRNA, *rpob1*, *rpob2*, and *gyrb* genes were amplified and sequenced, followed by phylogenetic tree construction based on NCBI alignment results, which revealed that this bacterium clustered with *A. ursingii* (Fig. 1C, D, S2). Therefore, combining morphological observation, biochemical identification, and molecular identification, this hemolytic *Acinetobacter* strain was identified as *A. ursingii*. The 16 S rRNA gene sequence of *A. ursingii* 31C2 has been submitted to the National Center for Biotechnology Information (NCBI), with the accession number of PQ248402, and its specific sequencing data has been registered in the GenBank database.

The Pathogenicity of *A. ursingii* 31C2

The swimming ability of shrimp infected with *A. ursingii* 31C2 was weakened. Continuous observation of mortality of shrimp at 96 h after infection showed that at a dose of 4.16×10^4 CFU/g shrimp body weight, the mortality rate was only 15%. However, increasing the dose by one or two orders of magnitude significantly led to significant shrimp mortality, showing a dose-dependent effect. Infection with 4.16×10^5 CFU/g of shrimp body weight resulted in mortality rates of 50%, 70%, and 90% at 24, 48, and 96 h, respectively. Infection with 4.16×10^6 CFU/g of shrimp body weight resulted in mortality rates of 60%, 90%, and 100% at 24, 48, and 96 h, respectively (Fig. 2A). Dissection of freshly dead shrimp revealed no abnormalities in Group A, with intact hepatopancreas structure and normal appearance of the intestine. Shrimp in Group B showed redness in the tail fan and swimming legs, partial necrosis and lysed hepatopancreas, and redness of the intestine; shrimp in Group D exhibited redness in the tail fan and swimming legs, almost complete necrosis and lysed hepatopancreas, and partially lysed intestine, which became brittle and lacked intact structure (Fig. 2B). *A. ursingii* 31C2 was successfully re-isolated from the hepatopancreas, intestine, and gills of the infected

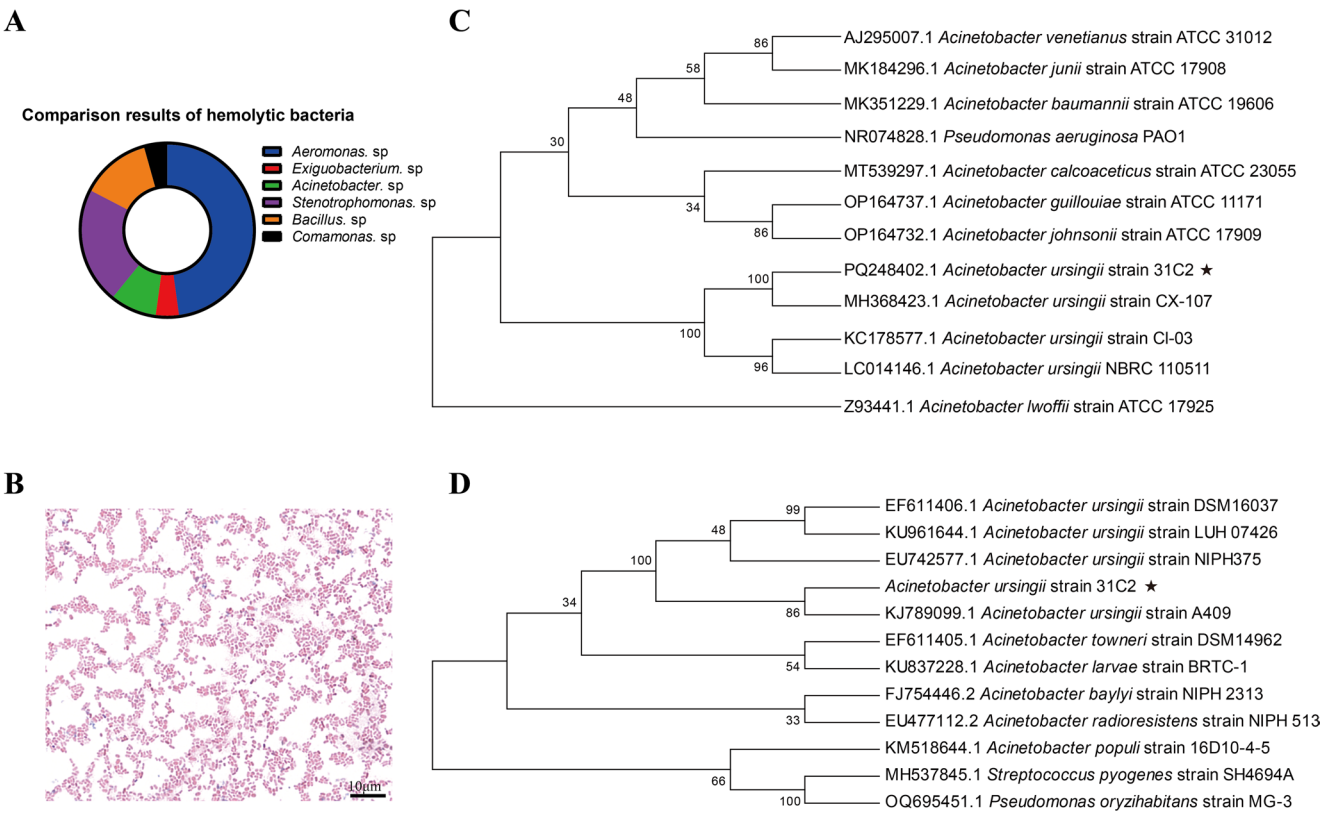

Fig. 1 Isolation and identification of potential pathogenic bacteria from*L. vannamei.* (**A**) Based on the results of 16 S rRNA sequencing, 119 strains derived from shrimp were identified and classified at the genus level. (**B**) The potential pathogen *A. ursingii* 31C2 underwent Gram staining. A phylogenetic tree was created to analyze the evolutionary relationships of *A. ursingii* 31C2 with other species, utilizing the 16 S rRNA sequence (**C**) and the *rpob1* sequence (**D**). This analysis was conducted using the N-J tree method within the MEGA 6.0 software package, employing 1,000 bootstrap replicas

Table 1 Biochemical identification of 31C2

Biochemical detection index	Purified strain 31C2
Glucose	-
Lactose	-
Maltose	-
Cane sugar	-
Mannose	-
Mannitol	-
Arabinose	-
Nitrate reduction	-
Simmons citrate agar	+
Esculin	-
Gelatin	-
Hydrogen sulfide	-
Urea	-
Phosphate glucose peptone water (MR)	-
Phosphate glucose peptone water (VP)	-
Semi-solid Agar	-
Oxidase	-
Catalase	+

shrimp, with significantly higher intestinal bacterial load than in the gills and hepatopancreas (Fig. 2C). The 48 h and 96 h LD_{50} values for shrimp infected with *A. ursingii* 31C2 were calculated using the modified Karber method, which was 1.09×10^4 CFU/g of shrimp body weight and 2.83×10^4 CFU/g of shrimp body weight, respectively. The artificially infected shrimp exhibited similar external signs to those observed in the naturally diseased individuals, including reduced activity, body discoloration, and partial hepatopancreatic erosion (Fig. S1). These consistent macroscopic manifestations verified that the *A. ursingii* 31C2 challenge model successfully reproduced the natural infection, confirming its pathogenicity in *L. vannamei*.

To further understand the pathogenicity of *A. ursingii* 31C2, the marine model species, *O. melastigma*, was used for infective injection. It was found that an infective dose of 8.8×10^3 CFU/fish did not cause mortality in *O. melastigma* within 96 h, whereas an increase of the dose by one order of magnitude resulted in only 10% mortality, and an

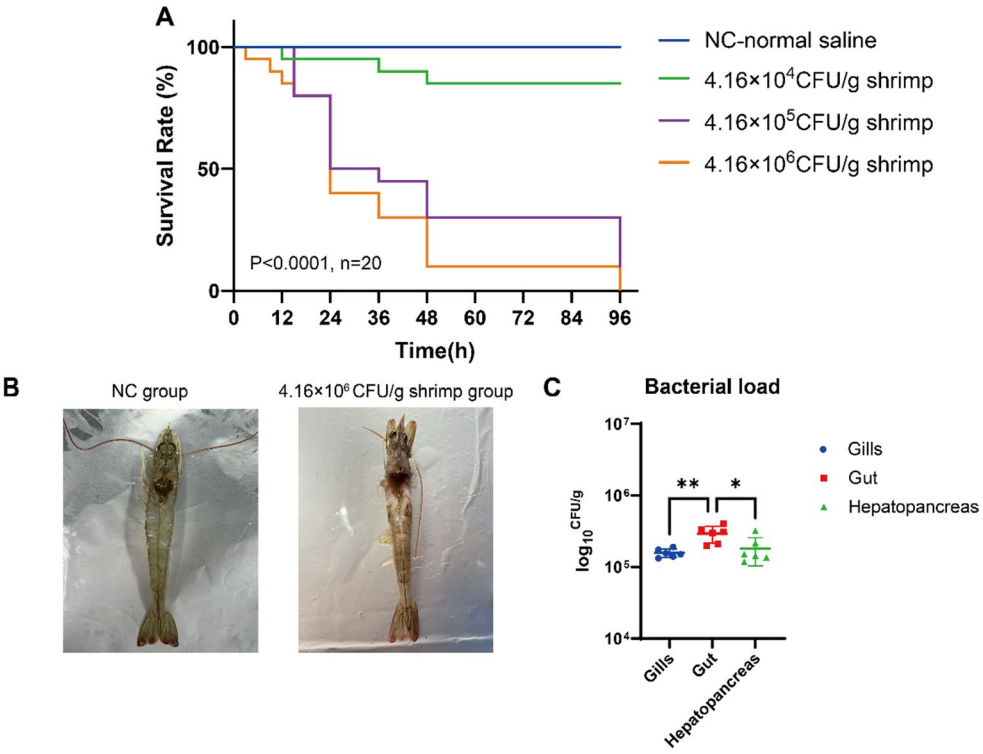

Fig. 2 Assessment of Pathogenicity of *A. ursingii* 31C2 in *L. vannamei* (A, B, C). (**A**) *L. vannamei* were intraperitoneally infected with 4.16×10^4 CFU/g, 4.16×10^5 CFU/g, and 4.16×10^6 CFU/g of *A. ursingii* 31C2. The survival rates were monitored over a period of 96 h, and the survival curve was evaluated through the log-rank Mantel-Cox test ($n = 20$). (**B**) Visible pathological clinical signs observed in *L. vannamei* infected with *A. ursingii* 31C2. (**C**) Bacterial counts in the hepatopancreas, gut, and gill tissues of *L. vannamei* following a high dose of *A. ursingii* 31C2 infection. $^*p < 0.05$, $^{**}p < 0.01$

increase of two and three orders of magnitude led to 43.33% and 50% mortality of *O. melastigma*, respectively. After infection with 8.8×10^7 CFU/fish *A. ursingii* 31C2, all the *O. melastigma* died within 96 h (Fig. S3A), and showed obvious pathological symptoms, mainly characterized by abdominal swelling, redness and swelling of the gills, and the appearance of hemorrhagic spots of varying sizes on the body surface (Fig. S3B). *A. ursingii* 31C2 was also successfully re-isolated from the livers, gills and intestines of the infected *O. melastigma*, but there was no significant difference in the bacterial load among the three tissues (Fig. S3C). The 48 h and 96 h LD_{50} values of *O. melastigma* infected with *A. ursingii* 31C2 were 2.10×10^5 CFU/fish and 2.58×10^6 CFU/fish, respectively.

The results indicated that *A. ursingii* 31C2 was pathogenic to both *L. vannamei* and *O. melastigma*, and high-dose injective infections resulted in mortality in both aquatic animals.

Drug Susceptibility Test of *A. ursingii* 31C2

The results of drug sensitivity test indicated that *A. ursingii* 31C2 was sensitive to Imipenem, Amikacin, Ampicillin-sulbactam, Levofloxacin, Meropenem, Amoxicillin, Gentamicin, and Tobramycin, but resistant to Ampicillin, Oxacillin, Azithromycin, Cefotetan, Compound sulfamethoxazole, Rifampin, Piperacillin, Polymyxin B, Florfenicol, Aztreonam, Tetracycline, and Cefoxitin (Table 2).

Table 2 Drug sensitivity test of *A. ursingii* 31C2

Antibiotic	Inhibition zone (mm)				Sensitivity
	1	2	3	Mean	
Ampicillin	\	\	\	\	
Oxacillin	\	\	\	\	
Azithromycin	\	\	\	\	
Cefotetan	\	\	\	\	
Compound sulfamethoxazole	\	\	\	\	
Rifampin	\	\	\	\	
Imipenem	32	33	32	32.33	S
Amikacin	26	27	27	26.67	S
Ampicillin-Sulbactam	25	25	25	25.00	S
Levofloxacin	23	24	23	23.33	S
Meropenem	23	24	24	23.67	S
Amoxicillin	21	20	19	20.00	S
Gentamicin	21	22	22	21.67	S
Piperacillin-Tazobactam	20	21	19	20.00	I
Tobramycin	20	20	20	20.00	S
Ceftriaxone	16	16	17	16.33	I
Ceftazidime	15	14	15	14.67	I
Piperacillin	15	16	15	15.33	R
Cefepime	15	14	17	15.33	I
Polymyxin B	15	15	15	15.00	R
Florfenicol	14	14	14	14.00	R
Aztreonam	11	10	10	10.33	R
Tetracycline	11	12	11	11.33	R
Cefoxitin	10	11	10	10.33	R

Note: "\" indicates no inhibition zone observed (completely resistant); S, sensitive; I, intermediate; R, resistant

Antibacterial Activity of AMPs against *A. ursingii* 31C2

The results of antibacterial activity of the four AMPs against *A. ursingii* 31C2 were shown in Table 3. Scygonadin and Spgillcin$_{177-189}$ showed no obvious antibacterial activity against *A. ursingii* 31C2 at concentrations up to 48 μM. The MIC value of Bolespleenin$_{334-347}$ was 6–12 μM and the MBC value was 12–24 μM, while Scymicrosin$_{7-26}$ had both MIC and MBC of 3–6 μM, exhibiting the best inhibitory effect. Further SEM results showed that the untreated *A. ursingii* had a short rod shape (Fig. 3A), and after treatment with 3 μM Scymicrosin$_{7-26}$, the morphology and size of *A. ursingii* changed, with severe shrinkage and indentations, partial damage, and slight leakage of the cellular contents (Fig. 3B). Considering the strong bactericidal ability of Scymicrosin$_{7-26}$ against *A. ursingii* 31C2, Scymicrosin$_{7-26}$ was used for subsequent in vivo anti-infection tests.

The Anti-infective Effect of Scymicrosin$_{7-26}$ on *L. vannamei* Infected with *A. ursingii* 31C2

The AMP Scymicrosin$_{7-26}$ showed significant antibacterial activity against *A. ursingii in vitro*. To further explore its in vivo anti-infective effects, an injective infection was performed on shrimp using the 48 h LD_{50}, followed by the injection of Scymicrosin$_{7-26}$ to evaluate the peptide's in vivo anti-infective capabilities (Fig. 4A). Scymicrosin$_{7-26}$ significantly enhanced the survival rate of *A. ursingii*-infected shrimp by 30% compared to the infected group (Fig. 4B), while concurrently inducing statistically significant reductions in bacterial burden across all timepoints (3–48 h) and tissues. Hepatopancreas clearance ranged from 35.24% to 96.24%, with intestinal clearance reaching 74.77%−99.07% (Fig. 4C-D).

Pathological section observations at 3, 6, 9, 12, 24, and 48 h post-infection indicated that the microstructures of the hepatopancreas and intestine of *L. vannamei* underwent significant changes after infection (Fig. 5 and Fig. 6). The healthy hepatopancreas of the NC group was densely structured, with intact tubular structures, clear boundaries, and even distribution of secretory, fibroblastic, and absorptive cells. In contrast, the hepatopancreas of the shrimp infected with *A. ursingii* appeared to be damaged, with disordered arrangement of hepatic tubules, severe deformation of tubular lumens, enlarged intercellular spaces, blurred boundaries, severe darkening of cells and varying degrees of vacuolation in the epithelial cytoplasm. The damage to the hepatopancreas worsened over time, but after treatment with Scymicrosin$_{7-26}$ the damage caused by the infection was significantly alleviated (Fig. 5). The intestinal epithelial cells and microvilli of the NC group were intact and neatly arranged. After infection with *A. ursingii*, the intestinal tissue of the shrimp showed obvious damage, with shortening, shedding, and disappearance of intestinal villi, loosely arranged epithelial cells, detachment from the mucosal layer, and vacuolization in the muscle layer. After treatment with Scymicrosin$_{7-26}$, the intestinal mucosal damage was repaired, and the structure of the infected intestinal tissue remained basically intact (Fig. 6).

The temporal expression of immune-related genes in *A. ursingii*-infected shrimp hepatopancreas and intestine was analyzed following Scymicrosin$_{7-26}$ treatment (Fig. 7A and P). During early infection (3–6 h), genes of the canonical innate immune pathways—*toll*, *dorsal*, *imd*, and *relish*—were strongly induced in both the hepatopancreas (Fig. 7A

Table 3 Antibacterial activity of four novel peptides against *Acinetobacter ursingii* 31C2

Peptides	MIC (μM)	MBC (μM)
Scygonadin1	>48	>48
Spgillcin$_{177-189}$	>48	>48
Bolespleenin$_{334-347}$	6–12	12–24
Scymicrosin$_{7-26}$	3–6	3–6

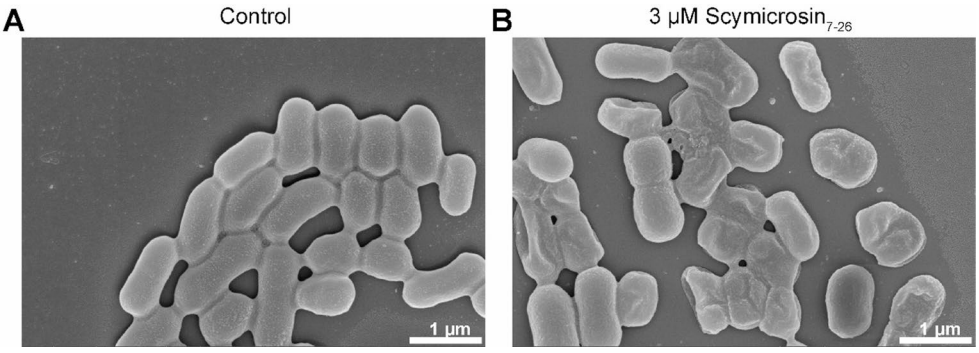

Fig. 3 Morphological alterations of *A. ursingii* 31C2 cells induced by the peptide Scymicrosin$_{7-26}$. (**A**) Scanning electron micrograph of untreated *A. ursingii* 31C2 cells showing intact and smooth surfaces. (**B**) Cells treated with 3 μM Scymicrosin$_{7-26}$ exhibited membrane disruption, deformation, and leakage of intracellular contents

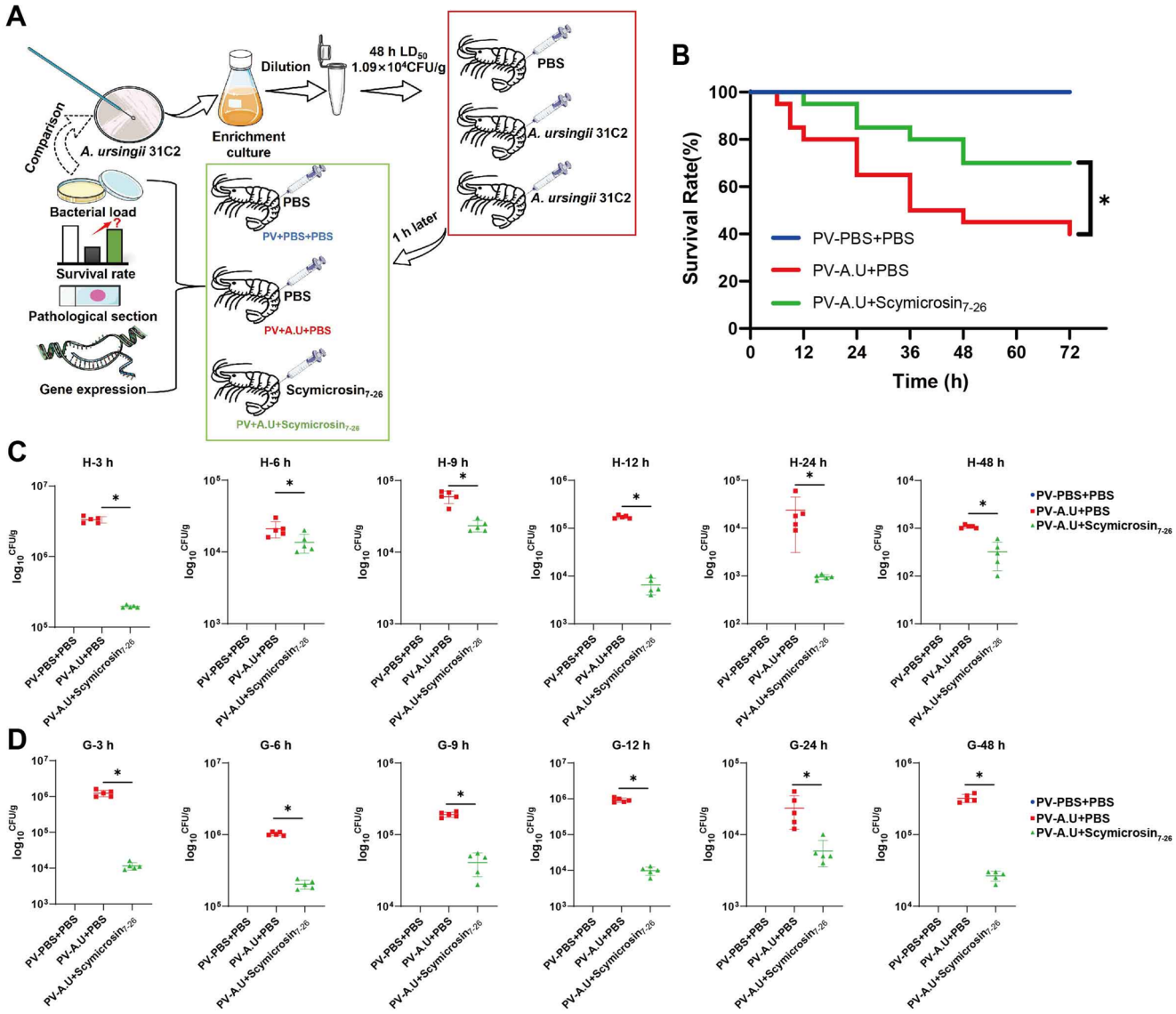

Fig. 4 The protective effect of Scymicrosin$_{7–26}$ on *L. vannamei* infected with *A. ursingii* 31C2. (**A**) Overall trial design. (**B**) The survival curves. The survival rates were monitored over a period of 72 h, and the survival curve was evaluated through the log-rank Mantel-Cox test ($n=30$). Bacterial loads in the hepatopancreas (**C**) and intestines (**D**) of three shrimp groups following infection with *A. ursingii* 31C2 at various time intervals (3–48 h). An asterisk signifies significant differences, $*p<0.05$. The bars illustrate the mean ± standard error of the mean ($n=5$)

and D) and intestine (Fig. 7I and L). Hepatopancreatic *toll* and *imd* peaked at 3 h, while *dorsal* and *relish* maintained high expression up to 6 h, indicating early activation of the Toll and IMD signaling cascades. In contrast, Scymicrosin$_{7–26}$ markedly suppressed this hyperactivation, reducing the expression of these genes at 3–6 h in both tissues, demonstrating an immunomodulatory effect that alleviated infection-induced inflammation. Antimicrobial peptides (AMPs) exhibited distinct temporal and tissue-specific responses. In the hepatopancreas, the expression of *penaeidin3*, *alf*, and *crustin* were rapidly upregulated at 3 h (Fig. 7E and G) but declined thereafter, whereas expression *propo* remained moderately elevated until 12 h (Fig. 7H). In the intestine, *penaeidin3*, *alf*, and *crustin* showed sustained expression from 6 to 24 h (Fig. 7M and O), with *propo* reaching a secondary peak at 24 h (Fig. 7P). Following Scymicrosin$_{7–26}$ administration, *penaeidin3* expression was further enhanced in the hepatopancreas at 3 h and in

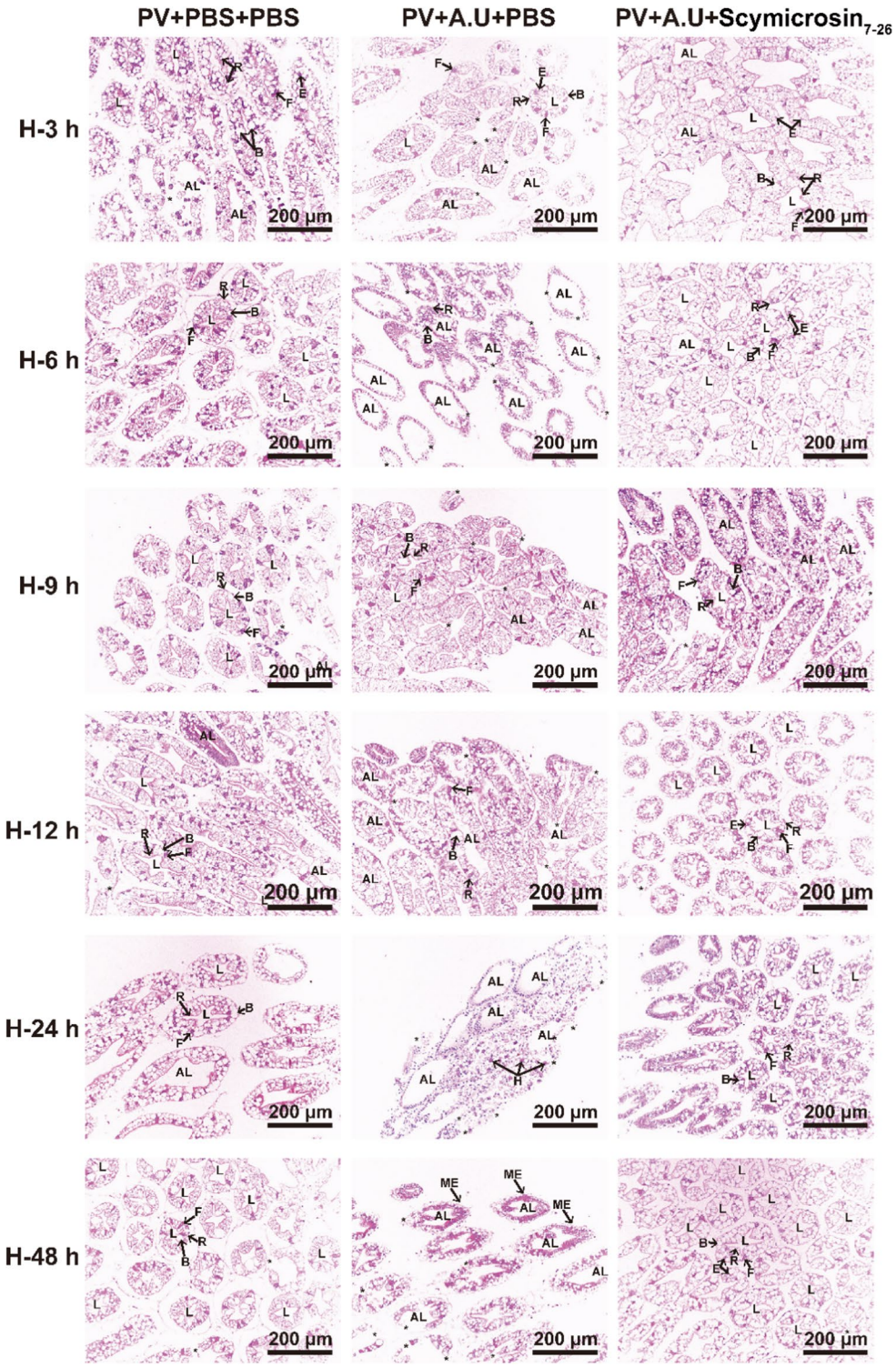

Fig. 5 The impact of Scymicrosin$_{7-26}$ on tissue architecture in the hepatopancreas of *L. vannamei* infected with *A. ursingii* 31C2. The tissue structure of the hepatopancreas in three groups of shrimp infected with *A. ursingii* 31C2 at various time points (3–48 h). In the figure, the letters and symbols represent the following: B (Blasenzellen, B cells), F (Fibrillazellen, F cells), R (Restzellen, R cells), E (Embryonalzellen, E cells), L (lumen), AL (abnormal lumen; irregular or expanded hepatopancreatic lumen compared with the normal pentagonal or quadrilateral structure), ME (melanization of cells), asterisk (*) (ruptured cells). H&E staining, magnification 100 times (100 ×), scale = 200 μm

the intestine at 24 h (Fig. 7E and M), while intestinal *crustin* and *propo* were significantly upregulated at 9 h and 24 h, respectively (Fig. 7O and P). These results suggest that Scymicrosin$_{7-26}$ restored effector gene activity during the later phase of infection and promoted prophenoloxidase system activation in a time-dependent manner.

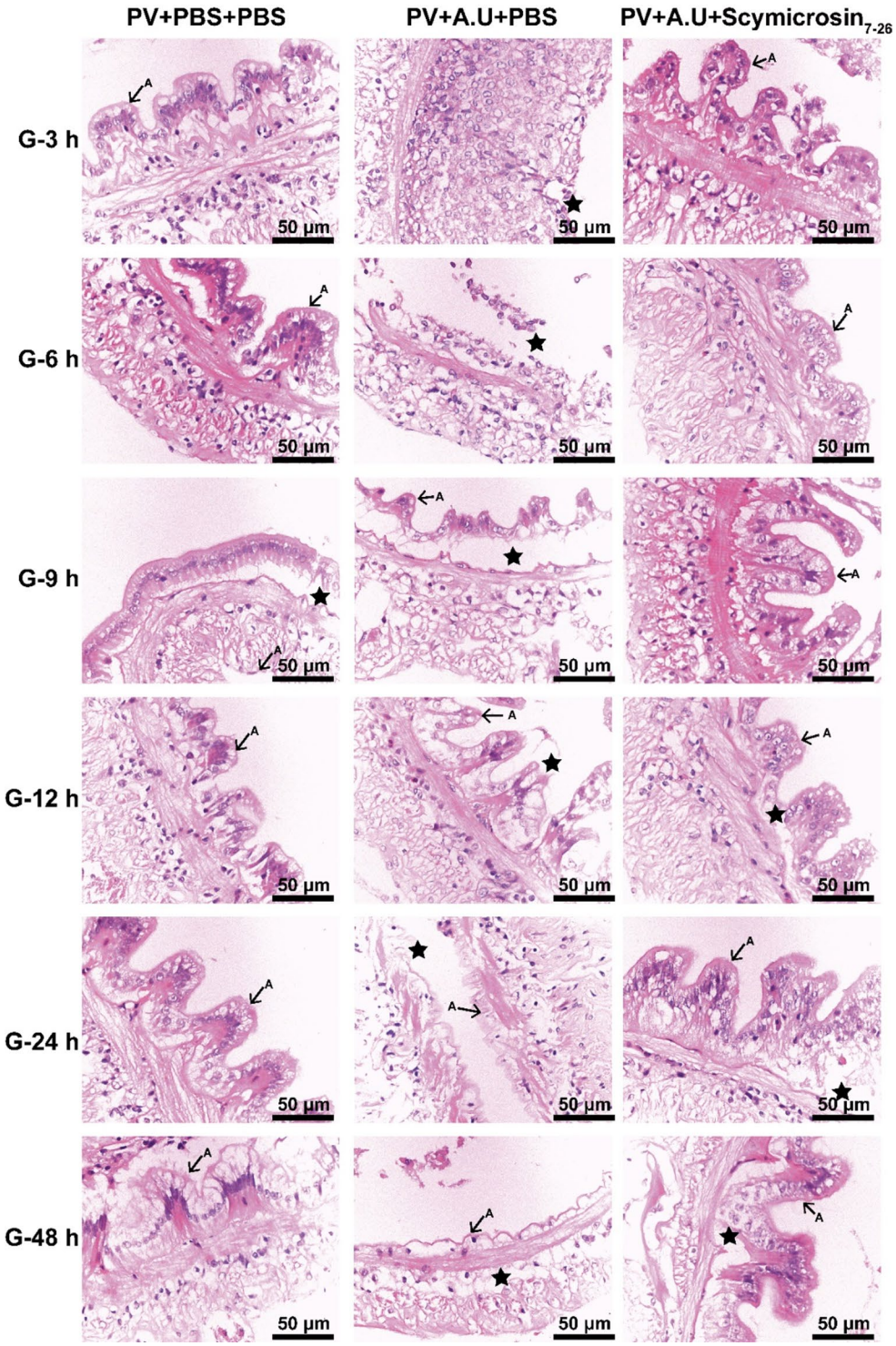

Fig. 6 The impact of Scymicrosin$_{7-26}$ on tissue architecture in the gut of *L. vannamei* infected with *A. ursingii* 31C2. The tissue structure of the intestines in three groups of shrimp infected with *A. ursingii* 31C2 at various time points (3–48 h). In the figure, the star symbol denotes damage to the intestinal structure, and the letter 'A' represents the intestinal villi. H&E staining, magnification 400 times (400 ×), scale = 50 μm

Collectively, Scymicrosin$_{7-26}$ conferred protection by dampening early pro-inflammatory signaling (3–6 h; Fig. 7A, D, I and L) and reactivating immune effector expression (*penaeidin3*, *crustin*, *propo*) during the recovery phase (12–48 h; Fig. 7E, H, M and P), thereby maintaining immune homeostasis and reducing mortality.

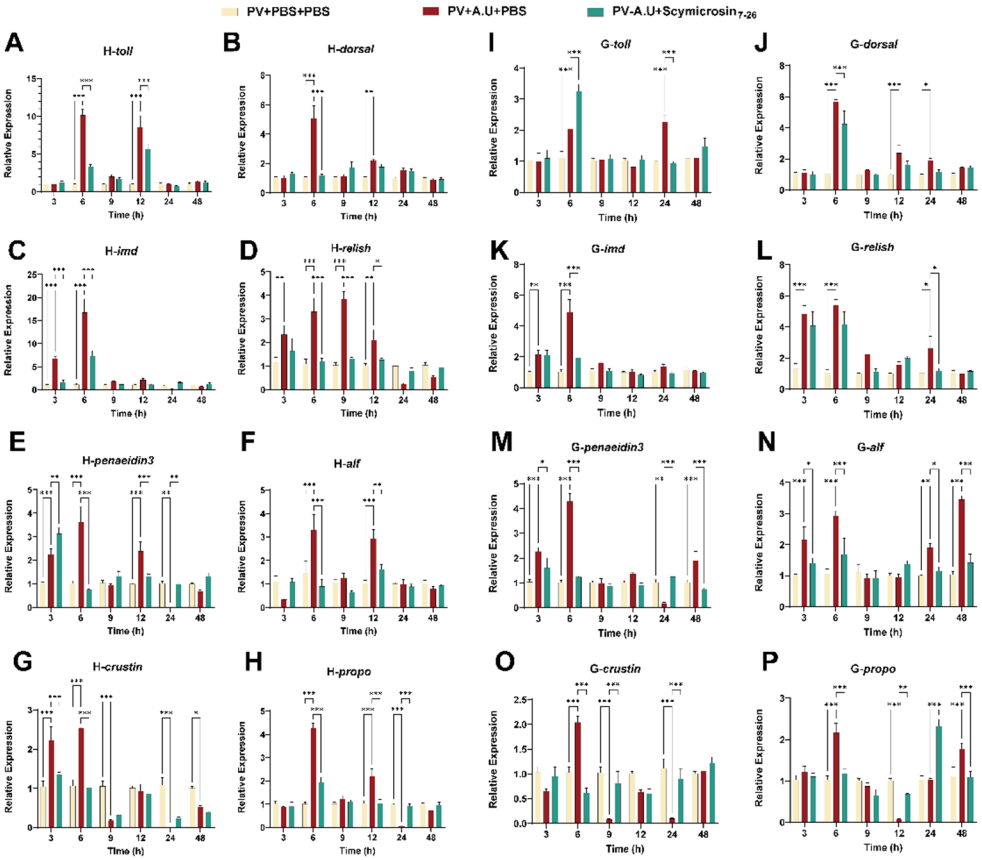

Fig. 7 The influence of Scymicrosin$_{7-26}$ on immune-related genes within the hepatopancreas (H) and intestinal (G) tract of *L. vannamei* infected with *A. ursingii* 31C2 was observed. (A-H) represent genes expressed in the hepatopancreas (H-*toll*, H-*dorsal*, H-*imd*, H-*relish*, H-*penaeidin*3, H-*alf*, H-*crustin*, and H-*propo*), (I-P) represent the corresponding intestinal genes (G-*toll*, G-*dorsal*, G-*imd*, G-*relish*, G-*penaeidin*3, G-*alf*, G-*crustin*, and G-*propo*). Significant differences are indicated by asterisks: $*p<0.05$, $**p<0.01$, $***p<0.001$. Bars represent mean ± SEM ($n=6$)

The Protective Effect of Scymicrosin$_{7-26}$ on *O. melastigma* Infected with *A. ursingii* 31C2

The in vivo anti-infective capability of the antimicrobial peptide Scymicrosin$_{7-26}$ was verified using the 48 h LD_{50} of *O. melastigma* for injective infection followed by an injection of Scymicrosin$_{7-26}$ (Fig. S4A). The results showed that Scymicrosin$_{7-26}$ significantly improved the survival rate of *O. melastigma* infected with *A. ursingii* by 20% compared with the infected group (Fig. S4B). Treatment with Scymicrosin$_{7-26}$ notably decreased the bacterial count in the liver and gut of female *O. melastigma* at both 24 and 48 h following infection with *A. ursingii* (Fig. S4C, S4D). Histopathological sections of the liver showed that in the NC group, the hepatocytes of *O. melastigma* were tightly arranged without obvious lesions (Fig. S4E). After 24 h of *A. ursingii* infection, the hepatocytes were loosely arranged with enlarged intercellular spaces, and as the infection time extended, by 48 h post-infection, the liver damage in *O. melastigma* was evident, with severe cell damage and rupture, further enlargement of intercellular spaces, and disappearance of normal cell morphology, which was alleviated by Scymicrosin$_{7-26}$ treatment (Fig. S4E). Compared with the NC group, both the infected group and the Scymicrosin$_{7-26}$ treated group showed an increase in goblet cells, intestinal villi damage, and thinning of the muscular layer at 24 h post-infection. At 48 h post-infection, the damage and shedding of intestinal villi in the infected group were exacerbated, whereas the intestinal histological structure was essentially normal in the Scymicrosin$_{7-26}$ treated group (Fig. S4F).

Discussion

L. vannamei is a cornerstone species in global aquaculture, yet its cultivation remains faced with challenges such as bacterial infections [43]. Typically, whiteleg shrimp are affected by bacterial diseases caused by hemolytic pathogens isolated from infected individuals [46, 47]. In the present study, *A. ursingii*, an *Acinetobacter* species, was isolated and identified for the first time from the intestine of diseased shrimp, representing the first report of this species in crustaceans. In most reports, *A. ursingii* has been described as widely present in the environment and is an opportunistic pathogen associated with skin colonization and bacteremia in hospitalized patients [23]. In recent years, reports of infections caused by this bacterium have begun to extend beyond humans; it can cause urinary tract

infections in dogs, as well as clinical signs such as tissue lesions and intestinal inflammation in rainbow trout [24, 25]. This finding suggests that *A. ursingii* possesses a broad host range and the capacity for cross-species transmission. Its detection in shrimp from Zhangpu County, Fujian Province, China, may be associated with anthropogenic contamination or environmental introduction from nearby aquaculture and residential areas. The Zhangpu farming area is located along a coastal estuarine zone that receives inputs from multiple sources, including riverine runoff, aquaculture effluents, and domestic sewage. Such conditions can facilitate the persistence and transmission of opportunistic bacteria like *A. ursingii* from terrestrial or human-associated reservoirs into marine culture systems. The widespread use of shared seawater intakes and the absence of closed biosecurity barriers may further increase the probability of bacterial colonization in shrimp ponds. This indicates that cross-species infections of this bacterium are occurring over time, and the bacterial infections could potentially cause significant economic losses to aquaculture industries [8, 10]. Therefore, continuous monitoring and research on emerging pathogens in aquatic species are extremely important. Enhanced disinfection of water sources, periodic microbial surveillance, and strengthened farm biosecurity management are recommended to minimize the risk of opportunistic bacterial outbreaks. The emergence of new pathogens can become an uncontrollable etiology leading to diseases and economic losses in aquatic animals. In addition, cross-species infections of zoonotic pathogens also pose a threat to public health. This study underscores the importance of such vigilance by identifying *A. ursingii* as a newly emerging pathogen in shrimp.

Some species in the genus *Acinetobacter* are emerging pathogens in aquaculture that can lead to substantial mortality in various aquatic species, including channel catfish (*Ictalurus punctatus*), blunt snout bream (*Megalobrama amblycephala*) and freshwater-cultured whiteleg shrimp (*Penaeus vannamei*) [46]. Identification of *Acinetobacter* species generally involves phenotypic, biochemical, and molecular biological methods, with molecular biological identification being more accurate [48, 49]. Nonetheless, as time passes, while the comparative examination of the 16 S rRNA gene remains a dependable marker for identifying *Acinetobacter* at the genus level because of the conserved sequences, challenges persist in distinguishing species due to the substantial homology present in these sequences [23, 50]. The *rpob* gene, a housekeeping gene in *Acinetobacter*, exhibits high intraspecific similarity and interspecific variability [17, 51]. In addition, the *gyrb* gene enables rapid and efficient identification of *Acinetobacter* species and confirms the phylogenetic relationships among species with higher accuracy [52, 53]. Therefore, in this study, after sequencing and comparative analysis of the 16 S rRNA gene of the isolated strains, the study amplified the zone 1 and zone 2 regions of the *rpob* gene and the *gyrb* gene. After sequencing, the study conducted species identification and combined with phenotypic and biochemical identification to comprehensively determine the isolated strain as *A. ursingii*.

Following the identification of this new shrimp pathogen, the study further assessed the *A. ursingii* 31C2 virulence. Animal challenge experiments with *L. vannamei* using the marine model *O. melastigma* confirmed dose-dependent mortality and tissue-specific pathology, that is, shrimp exhibited hepatopancreatic necrosis and intestinal fragility, while medaka displayed hemorrhagic lesions and visceral damage. Notably, these pathologies align with reported manifestations in other species: *A. ursingii* infection in *O. mykiss* caused intestinal inflammation and splenomegaly [25], and canine urinary tract infections featured similar epithelial damage [24]. In humans, bacteremia induced by this pathogen correlates with systemic inflammation [23]. This conserved tropism for epithelial and immune tissues across vertebrates and invertebrates suggests a similar pathogenic mechanism involving tissue invasion and inflammatory dysregulation. Quantitative LD_{50} assessment further substantiated the strain's broad host adaptability, underscoring its emergent threat to diverse aquatic systems and zoonotic potential. The significant mortality and pathology observed necessitate effective control measures, which are further complicated by antibiotic resistance issues.

In aquaculture industries, the usage of antibiotics has always been a topic of great concern. Improper use or overuse may lead to the emergence and spread of antibiotic-resistant bacteria, thus affecting human health and ecosystems. The drug sensitivity test results showed that *A. ursingii* 31C2 is resistant to several antibiotics, such as Cefepime, Polymyxin B, Aztreonam, Tetracycline, Florfenicol, Azithromycin, Piperacillin, and Rifampin. These resistances suggested that antibiotic use in aquaculture and general environmental contamination are contributing factors, which is supported by the frequent isolation of *A. ursingii* from hospital effluents and residential wastewater [23]. For instance, Tetracycline and Florfenicol are extensively used to treat vibriosis and enteritis [54]. Their high prevalence has driven widespread resistance via efflux pumps (*tet* genes) and enzymatic inactivation [55]. Azithromycin (a macrolide) targets *Streptococcus* and *Edwardsiella* infections, but its prophylactic use in hatcheries promotes ribosomal mutation (e.g., *erm* genes) and biofilm-mediated resistance [56]. Cefepime and Piperacillin (β-lactams) resistance correlates with overuse against *Aeromonas* infections, inducing extended-spectrum β-lactamase (ESBL) production [57]. Polymyxin B resistance may arise from its increasing use as a "last-resort" drug when other treatments

have failed, selecting for *mcr* gene-mediated membrane modification. Notably, the preventive use of antibiotics by livestock farms, such as Enrofloxacin (Fluoroquinolones) and Sulfonamides, has created a continuous selection pressure. Moreover, the high-density agricultural production method promotes the spread of pathogens, which accelerates the horizontal gene transfer of resistance determinants (e.g., plasmids carrying tetracycline, *floR*, and *qnr*) among aquatic bacteria. These results demonstrate that antibiotic resistance is an evolving challenge driven by empirical drug application, inadequate farmer education, and insufficient regulatory oversight. The sensitivity to certain antibiotics and resistance to others highlights the precarious nature of bacterial drug susceptibility profiles and underscores the imperative for novel antimicrobial strategies, such as immunostimulants or the AMPs evaluated in this study, alongside strict antibiotic stewardship [19, 26, 36].

Antimicrobial peptides are important components of the innate immune system and stand out as superior alternatives to conventional antibiotics. They exhibit a range of advantages, such as broad-spectrum antimicrobial potency, less possibility of inducing drug resistance, immune-modulating capabilities, promotion of wound healing, and bio-degradability. In this study, four novel marine-derived AMPs, including Scygonadin [34], Spgillcin$_{177-189}$ [35], Bolespleenin$_{334-347}$ [29], and Scymicrosin$_{7-26}$, were selected from previously characterized peptides based on their preliminary broad-spectrum efficacy and low cytotoxicity. Scymicrosin$_{7-26}$ is a cationic α-helical peptide consisting of 20 amino acids with a net positive charge of + 4 and moderate hydrophobicity. It was originally identified from *Scylla paramamosain* and exhibits a typical amphipathic structure that facilitates electrostatic binding to negatively charged bacterial membranes. Previous studies have demonstrated that Scymicrosin$_{7-26}$ rapidly permeabilizes and disrupts bacterial membranes, as confirmed by SYTOX Green uptake assays, confocal microscopy, and transmission electron microscopy showing membrane deformation and cytoplasmic leakage in methicillin-resistant *Staphylococcus aureus* [36]. Given these established findings, the potent inhibitory activity of Scymicrosin$_{7-26}$ against *A. ursingii* observed in the present study is most plausibly mediated through a similar membrane-disruptive mechanism rather than intracellular metabolic interference.

Given its potent in vitro activity, the therapeutic potential of Scymicrosin$_{7-26}$ was subsequently evaluated in vivo against *A. ursingii* 31C2 infection in shrimp. It is reported that infection of rainbow trout with *A. ursingii* K180411 can result in extensive necrosis and sloughing of the intestinal epithelium, accompanied by diffuse swelling and necrosis in the liver tissue [24, 25]. Similarly, it was observed that *A. ursingii* 31C2 infection induced significant tissue damage and a marked increase in bacterial load in shrimp. Concomitantly, genes associated with the immune response were significantly upregulated, indicative of a robust host defense reaction triggered by pathogen recognition (e.g., via PAMPs) and tissue damage (e.g., via DAMPs). Treatment with Scymicrosin$_{7-26}$ alleviated these pathological manifestations, including the immune gene dysregulation, tissue damage, and elevated bacterial burden.

To elucidate the underlying immune mechanisms modulated by Scymicrosin$_{7-26}$, key signaling pathways and effector molecules were analyzed. As the main signaling pathways in the innate immune system of shrimp, the Toll and IMD pathways play pivotal roles in pathogen recognition and the initiation of immune responses [58–60]. The *toll* receptor and the transcription factor *dorsal* are core components of the Toll pathway. Detection of pathogen-associated molecular patterns (PAMPs) by the *toll* receptor triggers downstream signaling cascades, culminating in the transcription of AMPs [61, 62]. The Toll pathway typically requires microbial ligands to interact with circulating recognition proteins (e.g., peptidoglycan recognition proteins, PRPs) for activation. In contrast, the IMD pathway is initiated more directly by the interaction of peptidoglycans (PGNs), particularly from Gram-negative bacteria and certain Gram-positive bacilli with meso-diaminopimelic acid-type (DAP-type) PGNs, with transmembrane receptors. Intracellular infection signals ultimately activate the NF-κB transcription factor *relish*, which translocates to the nucleus to regulate AMP synthesis [59, 62, 63]. In shrimp, a number of AMPs are present, including ALF, Crustin, and Penaeidin, which also play significant roles in the immune response. ALF contains a conserved lipopolysaccharide-binding domain (LBD) and activates the coagulation cascade by binding LPS, thereby exerting broad-spectrum antibacterial and antiviral activity [64]. Crustin and Penaeidin can target bacterial membranes and promote the phagocytosis of pathogens by hyaline cells through opsonization [65, 66]. Critically, these AMPs represent a frontline defense, and their expression is rapidly induced upon pathogen challenge, particularly in the early stages of infection. Consistent with this paradigm, studies have demonstrated significant upregulation of *alf*, crustin, and *penaeidin* transcripts in shrimp hepatopancreas and other tissues following exposure to bacterial pathogens (e.g., *Vibrio* spp.) and viruses like WSSV, often peaking within hours post-infection [63, 67–70]. The results revealed that *A. ursingii* infection triggered immediate upregulation of *imd*, *relish* and AMP genes (*penaeidin3*, *crustin*, *alf*) in hepatopancreas and intestine within 3–6 h, aligning with reports that *Vibrio* infections induce *penaeidin3* within 4 h and *alf* within 6 h [67, 69]. Notably, the subsequent

decline in *crustin* expression by 9 h and *penaeidin3* and *alf* fluctuations at 12–24 h suggest feedback regulation to prevent immune hyperactivation, corroborating observations that sustained AMP overexpression causes tissue damage in shrimp [59].

Interestingly, Scymicrosin$_{7-26}$ treatment attenuated this immune dysregulation. Its early induction of *penaeidin3* (3 h) preceded pathogen-triggered responses, potentially priming immune readiness. By 6 h, it significantly suppressed *toll*, *dorsal*, *imd*, *relish*, and AMPs (*alf*, *crustin*, *propo*), indicating modulation of both NF-κB pathways and downstream effectors. These findings parallel reports showing that cationic AMPs such as Scymicrosin$_{7-26}$ compete with host cationic proteins for binding to anionic PAMPs (e.g., LPS), thereby dampening TLR, *imd* overactivation [29, 36]. Melanization, a vital first line of innate defense regulated by the prophenoloxidase (*propo*) system, is a key component of shrimp humoral immunity [71–73]. The restoration of *propo* and *penaeidin3* levels at 24 h further demonstrates the peptide's role in rebalancing melanization and AMP synthesis—key mechanisms mitigating inflammation-induced mortality [73].

Taken together, the results testified that *A. ursingii* infection rapidly engages the Toll and IMD pathways, driving the characteristic early upregulation of AMPs like *alf*, *crustin*, and *penaeidin*, but also induces complex temporal shifts potentially indicative of immune stress or dysregulation. The efficacy of Scymicrosin$_{7-26}$ in reducing mortality may be attributed to its combined antimicrobial and immune-modulatory effects, as supported by the suppression of excessive inflammatory gene expression observed in vivo. By selectively attenuating the hyperactivation of key inflammatory signaling genes (*toll*, *imd*) and the excessive induction of AMPs and *propo* during the acute phase, Scymicrosin$_{7-26}$ appears to alleviate immunopathological damage associated with uncontrolled inflammation, contributing to improved survival outcomes. This modulation, coupled with its potential role in later-stage restoration of specific immune effectors like *penaeidin3*, positions Scymicrosin$_{7-26}$ as a valuable agent not only for its direct antimicrobial properties but also for its capacity to fine-tune the host immune response, promoting a more balanced and protective outcome against bacterial challenge. The validation experiments in the marine medaka also demonstrated that Scymicrosin$_{7-26}$ not only enhances the survival rate of the marine medaka, but also mitigates the liver and intestinal damage caused by *A. ursingii* 31C2 infection, and promotes the recovery of tissue structure. Consequently, Scymicrosin$_{7-26}$ holds significant promise as a potential antimicrobial agent for the prevention and treatment of bacterial diseases in aquaculture, thereby improving the survival and health status of cultured fish. Future studies would further investigate the efficacy of Scymicrosin$_{7-26}$ under various farming conditions, as well as its synergistic effects with other disease control measures.

Conclusions

In conclusion, this study establishes *A. ursingii* as a novel pathogenic bacterium in *L. vannamei*, demonstrating dose-dependent virulence in shrimp ($LD_{50}=2.83\times10^4$ CFU/g of shrimp body weight) and the model fish *O. melastigma* ($LD_{50}=2.58\times10^6$ CFU/fish), causing hepatopancreatic necrosis and intestinal lesions. The isolate exhibited multidrug resistance to 12 antibiotics, underscoring the urgency for alternatives. Among screened marine antimicrobial peptides, Scymicrosin$_{7-26}$ showed potent in vitro activity (MIC 3–6 μM) through membrane disruption and conferred significant in vivo protection—enhancing survival by 30% in shrimp and 20% in medaka while reducing bacterial loads by 35–99% in key tissues. Critically, it attenuated pathogenic inflammation by modulating Toll and IMD immune hyperactivation and restored effector gene expression (*penaeidin3*, *propo*), positioning it as a sustainable therapeutic candidate against emerging antibiotic-resistant pathogens in aquaculture.

Supplementary Information The online version contains supplementary material available at https://doi.org/10.1007/s12602-025-10866-y.

Acknowledgements We thanks to laboratory engineers Huiyun Chen, Ming Xiong, Hui Peng, and Zhiyong Lin for their valuable technical support.

Author Contributions Ying Wang : Data curation, Formal analysis, Methodology, Validation, Visualization, Writing - original draft, Writing - review & editing. Hanxiao Li : Data curation, Formal analysis, Investigation, Methodology. Hua Hao : Investigation, Methodology. Ying Zhou : Investigation, Methodology. Fangyi Chen : Conceptualization, Funding acquisition, Project administration, Resources, Supervision, Writing - review & editing. Ke-Jian Wang : Conceptualization, Funding acquisition, Project administration, Resources, Supervision, Writing - review & editing.

Funding This study was supported by grant FJHYF-L-2025-13 from Fujian Ocean and Fisheries Bureau; grant 2025N5001 from Fujian Province Industry-Academia Collaboration Project; grant 22CZP002HJ08 from Xiamen Ocean Development Bureau.

Data Availability No datasets were generated or analysed during the current study.

Declarations

Competing interests The authors declare no competing interests.

References

1. Ruan Y, Wong NK, Zhang X, Zhu CH, Wu XF, Ren CH et al (2020) Vitellogenin receptor (VgR) mediates oocyte maturation and ovarian development in the Pacific white shrimp (*Litopenaeus vannamei*). Front Physiol 11
2. FAO (2024) The state of world fisheries and aquaculture 2024. FAO
3. MARA (2024) China Fishery Statistical Yearbook. Beijing
4. Li HY, Li QY, Wang S, He JG, Li CZ (2023) Ammonia nitrogen stress increases susceptibility to bacterial infection via blocking IL-1R-Relish axis mediated antimicrobial peptides expression in shrimp. Aquaculture 563
5. Wang Y, Wang B, Liu M, Jiang K, Wang M, Wang L (2019) Comparative transcriptome analysis reveals the different roles between hepatopancreas and intestine of *Litopenaeus vannamei* in immune response to aflatoxin B1 (AFB1) challenge. Comp Biochem Physiol C: Toxicol Pharmacol 222:1–10
6. Huang Z, Chen Y, Weng S, Lu X, He J (2016) Multiple bacteria species were involved in hepatopancreas necrosis syndrome (HPNS) of *Litopenaeus vannamei*. Acta Sci Natur Univ Sunyatseni
7. Kumar BK, Deekshit VK, Raj JRM, Rai P, Shivanagowda BM, Karunasagar I et al (2014) Diversity of associated with disease outbreak among cultured (Pacific white shrimp) in India. Aquaculture 433:247–251
8. Cao HP, Wang HC, Yu JJ, An J, Chen J (2019) Encapsulated powder as a potential Bio-Disinfectant against whiteleg Shrimp-Pathogenic *Vibrios*. Microorganisms 7(8)
9. Lee CT, Chen IT, Yang YT, Ko TP, Huang YT, Huang JY et al (2015) The opportunistic marine pathogen vibrio parahaemolyticus becomes virulent by acquiring a plasmid that expresses a deadly toxin. Proc Natl Acad Sci USA 112(39):E5445–E
10. Huang ZJ, Zeng SZ, Xiong JB, Hou DW, Zhou RJ, Xing CG et al (2020) Microecological Koch's postulates reveal that intestinal microbiota dysbiosis contributes to shrimp white feces syndrome. Microbiome 8(1)
11. Hou DW, Huang ZJ, Zeng SZ, Liu J, Wei DD, Deng XS et al (2018) Intestinal bacterial signatures of white feces syndrome in shrimp. Appl Microbiol Biotechnol 102(8):3701–3709
12. Yang H, Gao XJ, Li X, Zhang HH, Chen N, Zhang YY et al (2018) Comparative transcriptome analysis of red swamp crayfish (*Procambarus clarkia*) hepatopancreas in response to WSSV and *Aeromonas hydrophila* infection. Fish Shellfish Immunol 83:397–405
13. Huang Y, Lou GG, Man Z, Xiao XC, Zhu XM, Guo YZ et al (2023) Dietary sodium benzoate improves growth, morphology, antioxidant capacity and resistance against *Aeromonas hydrophila* of Pacific white shrimp (*Litopenaeus vannamei*). Aquacult Rep 33
14. Meng X, Chen F, Xiong M, Hao H, Wang K-J (2023) A new pathogenic isolate of *Kocuria Kristinae* identified for the first time in the marine fish *Larimichthys Crocea*. Front Microbiol 14:1129568
15. Kim PS, Shin NR, Kim JY, Yun JH, Hyun DW, Bae JW (2014) *Acinetobacter apis* sp. nov. Isolated from the intestinal tract of a honey bee, *Apis mellifera*. J Microbiol 52(8):639–645
16. Jechalke S, Kopmann C, Richter M, Moenickes S, Heuer H, Smalla K (2013) Plasmid-mediated fitness advantage of in sulfadiazine-polluted soil. FEMS Microbiol Lett 348(2):127–132
17. Nemec A, Musilek M, Maixnerova M, De Baere T, van der Reijden TJK, Vaneechoutte M et al (2009) *Acinetobacter beijerinckii* sp. nov. And *Acinetobacter gyllenbergii* sp. nov. Haemolytic organisms isolated from humans. Int J Syst Evol Microbiol 59:118–124
18. Doi Y, Murray GL, Peleg AY (2015) *Acinetobacter baumannii*: evolution of antimicrobial Resistance-Treatment options. Semin Respir Crit Care Med 36(1):85–98
19. Lee YT, Kuo SC, Yang SP, Lin YT, Chiang DH, Tseng FC et al (2013) Bacteremic nosocomial pneumonia caused by *Acinetobacter baumannii* and *Acinetobacter nosocomialis*: a single or two distinct clinical entities? Clin Microbiol Infect 19(7):640–645
20. Freire MP, Garcia DD, Garcia CP, Bueno MFC, Camargo CH, Magri ASGK et al (2016) Bloodstream infection caused by extensively drug-resistant *Acinetobacter baumannii* in cancer patients: high mortality associated with delayed treatment rather than with the degree of neutropenia. Clin Microbiol Infect 22(4):352–358
21. Salzer HJF, Rolling T, Schmiedel S, Klupp EM, Lange C, Seifert H (2016) Severe Community-Acquired bloodstream infection with *Acinetobacter ursingii* in person who injects drugs. Emerg Infect Dis 22(1):134–137
22. Nemec A, De Baere T, Tjernberg I, Vaneechoutte M, van der Reijden TJK, Dijkshoorn L (2001) *Acinetobacter ursingii* sp. nov. And *Acinetobacter schindleri* sp. nov., isolated from human clinical specimens. Int J Syst Evol Microbiol 51:1891–1899
23. Chiu CH, Lee YT, Wang YC, Yin T, Kuo SC, Yang YS et al (2015) A retrospective study of the incidence, clinical characteristics, identification, and antimicrobial susceptibility of bacteremic isolates of *Acinetobacter ursingii*. BMC Infect Dis 15
24. Salavati S, Taylor CS, Harris JD, Paterson GK (2018) A canine urinary tract infection representing the first clinical veterinary isolation of *Acinetobacter ursingii*. New Microbes New Infect 22(C):4–5
25. Chunyan W, Siyu R, Kaiyu W, Huajing P, Isolation (2019) Identification and pathological infection lesions of *Acinetobacter ursingii* from rainbow trout *Oncorhynchus Mykiss*. Fish Sci 38(6):797–803
26. Zhang C, Chen FY, Bai YQ, Dong XX, Meng XZ, Wang KJ (2024) A novel antimicrobial peptide $Spasin_{141-165}$ identified from *Scylla paramamosain* exhibiting protection against *Aeromonas hydrophila* infection. Aquaculture 591:741137
27. Levy SB, Marshall B (2004) Antibacterial resistance worldwide: causes, challenges and responses. Nat Med 10(12):S122–S9
28. Tassanakajon A, Somboonwiwat K, Amparyup P (2015) Sequence diversity and evolution of antimicrobial peptides in invertebrates. Dev Comp Immunol 48(2):324–341
29. Bai YQ, Zhang WB, Zheng WB, Meng XZ, Duan YY, Zhang C et al (2024) A 14-amino acid cationic peptide $Bolespleenin_{334-347}$ from the marine fish *mudskipper boleophthalmus pectinirostris* exhibiting potent antimicrobial activity and therapeutic potential. Biochem Pharmacol 226
30. Shabir U, Ali S, Magray AR, Ganai BA, Firdous P, Hassan T et al (2018) Fish antimicrobial peptides (AMP'S) as essential and promising molecular therapeutic agents: A review. Microb Pathogen 114:50–56
31. Zasloff M (2002) Antimicrobial peptides of multicellular organisms. Nature 415(6870):389–395
32. Chaturvedi P, Bhat RAH, Pande A (2020) Antimicrobial peptides of fish: innocuous alternatives to antibiotics. Rev Aquacult 12(1):85–106
33. Wu D, Fu LL, Wen WZ, Dong N (2022) The dual antimicrobial and Immunomodulatory roles of host defense peptides and their applications in animal production. J Anim Sci Biotechnol 13(1)
34. Wang KJ, Huang WS, Yang M, Chen HY, Bo J, Li SJ et al (2007) A male-specific expression gene, encodes a novel anionic antimicrobial peptide, scygonadin, in *Scylla Serrata*. Mol Immunol 44(8):1961–1968
35. Wang XF, Hong X, Chen FY, Wang KJ (2022) A truncated peptide $Spgillcin_{177–189}$ derived from mud crab *Scylla paramamosain* exerting multiple antibacterial activities. Front Cell Infect Microbiol 12
36. Zhou Y, Wang Y, Meng XY, Xiong M, Dong XX, Peng H et al (2025) A newly identified antimicrobial peptide $Scymicrosin_{7-26}$ from *Scylla paramamosain* showing potent antimicrobial activity

against methicillin-resistant *Staphylococcus aureus in vitro* and *in vivo*. ACS Infect Dis 11(5):1216–1232
37. Wang J, Ruan Z, Feng Y, Fu Y, Jiang Y, Wang H et al (2014) Species distribution of clinical *acinetobacter* isolates revealed by different identification techniques. PLoS ONE 9(8):e104882
38. Holt JH, Krieg NR, Sneath PHA, Staley JT, Williams ST (1994) Bergey's manual of determinative bacteriology ninth edition. Bergey's manual of determinative bacteriology
39. Du H, Cai Y, Shen L, Zheng Y, Zhao L, Hu R et al (2025) *Bifidobacterium animalis sub*sp. Lactis modulates early-life immune response and gut metabolism. Anim Models Experimental Med 8(6):965–976
40. Li J, Qi Y, Song F, Dai F, Qiu T, Zhang X (2024) In-situ gelation of sodium Alginate-chitosan for oral delivery of probiotics. J Wuhan Univ Technology-Mater Sci Ed 39(6):1621–1627
41. Wang A-Z, Ma Q-X, Zhao H-J, Zhou Q-H, Jiang W, Sun J-Z (2012) A comparative study of the mortality rate of rats receiving a half lethal dose of fat intravenously: under general anaesthesia versus under spinal anaesthesia. Inj 43(3):311–314
42. CLSI (2022) Performance standards for antimicrobial susceptibility testing. Clinical and Laboratory Standards Institute, Wayne, PA
43. Daehyun K, Kyeong-Jun L (2024) Dietary vitamin C reduces mortality of Pacific white shrimp (Penaeus vannamei) post-larvae by vibrio parahaemolyticus challenge. Fish Shellfish Immunol 151(0)
44. Chomczynski P, Sacchi N (1987) Single-step method of RNA isolation by acid guanidinium thiocyanate–phenol–chloroform extraction. Anal Biochem 162(1):156–159
45. Livak KJ, Schmittgen TD (2002) Analysis of relative gene expression data using Real-Time quantitative PCR. Methods 25(4):402–408
46. Huang XD, Gu Y, Zhou HH, Xu L, Cao HP, Gai CL (2020) *Acinetobacter venetianus*, a potential pathogen of red leg disease in freshwater-cultured whiteleg shrimp *Penaeus vannamei*. Aquacult Rep 18
47. Flores-Miranda MD, Luna-González A, Córdova AIC, Fierro-Coronado JA, Partida-Arangure BO, Pintado J et al (2012) Isolation and characterization of infectious *Vibrio Sinaloensis* strains from the Pacific shrimp *Litopenaeus vannamei* (Decapoda: Penaeidae). Rev Biol Trop 60(2):567–576
48. Tarasevich IV, Shaginyan IA, Mediannikov OY (2010) Problems and perspectives of molecular epidemiology of infectious diseases. Ann Ny Acad Sci 990:751–756
49. Ruppitsch W, Stöger A, Indra A, Grif K, Schabereiter-Gurtner C, Hirschl A et al (2007) Suitability of partial 16S ribosomal RNA gene sequence analysis for the identification of dangerous bacterial pathogens. J Appl Microbiol 102(3):852–859
50. Janda JM, Abbott SL (2007) 16S rRNA gene sequencing for bacterial identification in the diagnostic laboratory: Pluses, perils, and pitfalls. J Clin Microbiol 45(9):2761–2764
51. La Scola B, Gundi VAKB, Khamis A, Raoult D (2006) Sequencing of the RpoB gene and flanking spacers for molecular identification of *Acinetobacter species*. J Clin Microbiol 44(3):827–832
52. Teixeira AB, Barin J, Hermes DM, Barth AL, Martins AF (2017) PCR assay based on the GyrB gene for rapid identification of *Acinetobacter baumannii*-calcoaceticus complex at specie level. J Clin Lab Anal 31(3)
53. Yamamoto S, Harayama S (1996) Phylogenetic analysis of *Acinetobacter* strains based on the nucleotide sequences of GyrB genes and on the amino acid sequences of their products. Int J Syst Bacteriol 46(2):506–511
54. Woo SJ, Kim MS, Jeong MG, Do MY, Hwang SD, Kim WJ (2022) Establishment of epidemiological Cut-Off values and the distribution of resistance genes in *Aeromonas hydrophila* and *Aeromonas veronii* isolated from aquatic animals. Antibiot (Basel) 11(3)
55. Miranda CD, Tello A, Keen PL (2013) Mechanisms of antimicrobial resistance in finfish aquaculture environments. Front Microbiol 4
56. Farrow KA, Lyras D, Rood JI (2000) The Macrolide-Lincosamide-Streptogramin B resistance determinant from *Clostridium difficile* 630 contains two erm(B) genes. Antimicrob Agents Chemother 44(2):411–413
57. Sekkin S, Kum C (2011) Antibacterial drugs in fish farms: application and its effects. Recent AdvFish Farms
58. Khush RS, Leulier F, Lemaitre B (2001) Drosophila immunity: two paths to NF-kappaB. Trends Immunol 22(5):260–264
59. Hong Q-M, Yang X-J, Zhang M-E, Chen Q, Chen Y-H (2024) Functional characterization of A deformed epidermal autoregulatory factor 1 gene in *Litopenaeus vannamei*. Dev Comp Immunol 151:105084
60. Hoffmann JA, Reichhart JM (2002) Drosophila innate immunity: an evolutionary perspective. Nat Immunol 3(2):121–126
61. Habib YJ, Wan HF, Sun YL, Shi JL, Yao CJ, Lin JM et al (2021) Genome-wide identification of toll-like receptors in Pacific white shrimp (*Litopenaeus vannamei*) and expression analysis in response to *Vibrio parahaemolyticus* invasion. Aquaculture 532
62. Wang PH, Liang JP, Gu ZH, Wan DH, Weng SP, Yu XQ et al (2012) Molecular cloning, characterization and expression analysis of two novel tolls (LvToll2 and LvToll3) and three putative Sptzle-like toll ligands (LvSpz1-3) from *Litopenaeus vannamei*. Dev Comp Immunol (2):36
63. Tassanakajon A, Rimphanitchayakit V, Visetnan S, Amparyup P, Somboonwiwat K, Charoensapsri W et al (2018) Shrimp humoral responses against pathogens: antimicrobial peptides and melanization. Dev Comp Immunol 80:81–93
64. Destoumieux-Garzón D, Rosa RD, Schmitt P, Barreto C, Vidal-Dupiol J, Mitta G et al (2016) Antimicrobial peptides in marine invertebrate health and disease. Philos T R Soc B 371:1695
65. Muñoz M, Vandenbulcke F, Saulnier D, Bachère E (2002) FEBS press. Eur J Biochem 269(11)
66. J S, R N, B V. (2015) Purification and characterization of a Cysteine-Rich 14-kDa antibacterial peptide from the granular hemocytes of Mangrove crab *Episesarma tetragonum* and its antibiofilm activity. Appl Biochem Biotechnol 176(4)
67. Li CZ, Wang S, He JG (2019) The two NF-κB pathways regulating bacterial and WSSV infection of shrimp. Front Immunol 10
68. Li FH, Xiang JH (2013) Signaling pathways regulating innate immune responses in shrimp. Fish Shellfish Immunol 34(4):973–980
69. Gu YL, Zhu L, Wang XR, Li H, Hou LB, Kong XH (2023) Research progress of pattern recognition receptors in red swamp crayfish (*Procambarus clarkii*). Fish Shellfish Immunol 141
70. Wang DD, Li FH, Li SH, Wen R, Xiang JH (2012) Expression profiles of antimicrobial peptides (AMPs) and their regulation by relish. Chin J Oceanol Limnol 30(4):611–619
71. Cerenius L, Lee BL, Söderhäll K (2008) The proPO-system: pros and cons for its role in invertebrate immunity. Trends Immunol 29(6):263–271
72. Söderhäll K, Cerenius L (1998) Role of the prophenoloxidase-activating system in invertebrate immunity. Curr Opin Immunol 10(1):23–28
73. Amparyup P, Charoensapsri W, Tassanakajon A (2013) Prophenoloxidase system and its role in shrimp immune responses against major pathogens. Fish Shellfish Immunol 34(4):990–1001